Deep Learning-Based Lung Tumor Analysis for Enhanced Oncology Diagnostics

G. Rohini Phaneendra Kumari
Department of IT
Vignan's Nirula Institute of Technology and Science for Women, Palakaluru, Guntur
ginjupallirohini@gmail.com

G. Akhila Reddy
Department of IT
Vignan's Nirula Institute of Technology and Science for Women, Palakaluru, Guntur
akhilareddygangireddy@gmail.com

Sk. Nazarana
Department of IT
Vignan's Nirula Institute of Technology and Science for Women, Palakaluru, Guntur
shaiknazarana@gmail.com

K. Vanaja
Department of IT Vignan's Nirula Institute of Technology and Science for Women, Palakaluru, Guntur
vanajakurra02@gmail.com

V. Snehitha
Department of IT
Vignan's Nirul Institute of Technology and Science for Women, Palakaluru, Guntur
Velugurisnehitha7@gmail.com

Naresh Alapati
Department of CSE
Vignan's Nirula Institute of Technology and Science for Women, Palakaluru, Guntur
alapatinaresh13@gmail.com

1.Abstract

Lung tumor analysis has become very instrumental this may involve earlier detection and treatment of lung cancer; hence, advanced computational methods must be employed to ascertain accurate diagnostics. The paper compares three deep learning algorithms performance: ResNet-50., U-Net, and VGG-16, for their effectiveness toward improving the accuracy, precision, recall, and F1 score of lung tumor detection. It exploits the deep residual learning framework of ResNet-50, the superior image segmentation capabilities of U-Net, and VGG-16's robust convolutional architecture for the development of an End-to-End System for the Analysis of Lung Tumors. In this paper, it will also demonstrate the computational efficiency of these algorithms in proving applicability in real clinical practice. Experimental results demonstrate that incorporating these algorithms significantly enhances diagnostic metrics to obtain a reliable and efficient solution for the detection of lung tumors. It is also concluded through this research that ResNet-50, U-Net, and VGG-16 combined together have greatly improved computational oncology by offering correct and reliable lung tumor diagnostics, very vital in effective management and treatment planning.

Keywords

Lung tumor analysis, ResNet-50, U-Net, VGG-16, deep learning, accuracy, precision, recall, F1 score, computational efficiency, image segmentation, oncology diagnostics.

2. Introduction

Lung cancer death is still on the top in terms of overall cancer deaths by country. NSCLC is the most common, including major subtypes such as adenocarcinoma and squamous cell carcinoma. Histological phenotype may have a major role in predicting the response to therapy and clinical outcome. Inherent to conventional light microscopy-based manual tissue assessment is its reliability, but interand intra-tumor heterogeneity cannot be captured often by biopsy procedures to present a complete disease profile. This can be further complemented by molecular testing in an attempt to identify distinct oncogenic driver mutation profiles; however, the adoption of this combination is hindered due to a lack of expertise and high costs associated with it.

Deep learning advancements in the recent past have shown some promise in addressing these challenges. The U-Net is a very effective model in the segmentation of medical images. One of the main reasons may be that its architecture was intended for biomedical image segmentation and, therefore, it can outline lung tumors effectively on CT and other imaging modalities. Having learned from a large amount of data, U-Net could provide detailed segmentations essential for accurate diagnosis and treatment planning, improving the understanding of tumor morphology.

Another deep learning adaptation is VGG-19, which has been used on a number of medical image classification tasks, including that pertaining to lung tumors. Using deep convolutional layers, VGG-19 can pick up minute features of the medical images, distinguishing between benign and malignant tumors. With such depth, VGG-19 lets one recognize complex patterns not visible by other methods, hence allowing higher accuracy for the diagnosis of lung cancer.

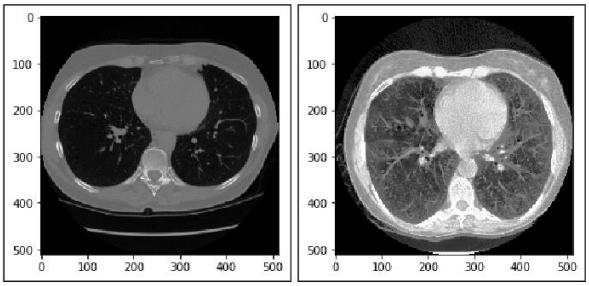

Fig1 Lung Tumor Detection

Powered by its very own residual learning framework, ResNet is quite effective in training very deep networks because it reduces the vanishing gradient problem. In lung tumor analysis, some variants of this examination, such as ResNet-50 and ResNet-101, are used in the detection and classification of lung cancers based on medical images with capacity to learn from deep representations of data, ResNet identifies very fine differences in tumor characteristics that aid in more accurate diagnosis and better-informed treatment decisions.

These deep learning algorithms have been applied to radiomics, and have changed the sphere of lung cancer analysis. Radiomics is a procedure for the extraction of quantitative features from medical images that characterizes tumor phenotypes. Deep learning allows automatic learning of such features from data and, therefore, makes the models more robust and predictive in nature. This approach has illustrated important potential in patient stratification and the prediction of clinical outcomes, therefore supporting personalized treatment strategies.

It has been shown to have an efficacy of deep learning in improving clinician accuracy and productivity. For instance, CNN-derived CT radiomic features have been correlated with specific biological and diagnostic patterns in lung cancer patients. The features can act like non-invasive biomarkers informative of tumor microanatomy, hence consequently help classification at early stages of NSCLC. Such innovative developments prove the potential of deep learning-based radiomics in supplementing conventional pathology workflows so as to get a complete overview of characteristics of the disease.

Deep learning algorithms like U-Net, VGG-19, and ResNet demonstrate a slightly bright potential for integration into lung tumor analysis to enhance diagnostic accuracy and treatment outcomes. Such models could be able to improve the work of pathologists and oncologists by automating the extraction and interpretation of complex features from medical images. Research will be pursued in this arena to keep boosting complex, cost-effective deep-learning models in the diagnosis and management of lung cancer, for betterment in patient care.

3.Literature Review

In this study, Q. -L. Lian, X. -Y. Li et al. [1] presented a method for diagnosing lung tumors in nude mice that combines laser-triggered breakdown spectroscopy with the histogram of the orientation process Changes and a Support Vector Machine. The method begins by acquiring elemental spectral lines and imaging maps for lung cells using the LIBS system. Then, the HOG is used to derive the gradient strategy relationship of multiple dimensions spectral magnitude from LIBS images. The optimal spectral features for each biological tissue are extracted based on the HOG. Finally, the SVM model is employed to detect lung tumors.

H. Hu, Q. Li et al[2]., Medical images are more and more crucial in clinical treatment. When diagnosing lung disease, clinicians rely heavily on imaging studies. Accurate removal of a tumor, particularly in surgical patients, requires complete knowledge of the tumor's size, location, and amount. Because of the volume of lung tumor images, computer-aided diagnosis is crucial for their analysis and therapy. This study presents a concurrent deep learning system that uses a hybrid mechanism of attention to segment images of lung tumors; the goal is to achieve complicated and self-adaptive segmentation.

In the process of cancer diagnosis and cure, the boundary of tumors needs to be elucidated. H. Hu, Q. Li et al [3]. proposed a new label-free imaging way for diagnosis in clinical lung cancer tissues. In this work, LIBS imaging was used to simultaneously obtain heterogeneity information of three types of clinical samples containing varying percentages of malignant tissue, and molecular fragments and more.

(H. Ladjal, M. Beuve, and others) [4]., A novel approach to tracking lung tumors that involves simulating the actual non-reproducible motion with a patient-specific biomechanical simulation of respiratory motion physiology. This will be propelled by movements that mimic the diaphragms and intercostal muscles, which are involved in breathing. How is this accomplished? By using surrogate measurements of the patient's rib cage kinematics and lung pressure to determine the volume relationship over a breath cycle. When optimizing lung pressure, finite helix axis computation is employed, and when computing rib displacement, inverse analysis of finite elements is employed. to minimize errors in lung volume. The amplitude of breathing motion in 4D CT scans was

well estimated by the system at an average landmark error of 2.0±1.3 mm.
The applicability of a new deep learning network in 2-D tumor trajectory estimation in fluoroscopic images. T. Peng, Z. Jiang et al[5]., With the use of generative adversarial approaches utilizing a coarse-to-fine architecture using convolutional LSTM modules, periodic tumor movements can be captured. Prepared and evaluated using a computerized X-CAT phantom, this model has been able to predict localized tumor regions for every phase of the breathing cycle. Two studies were performed: one on how accuracy changes concerning phantoms of different scales, tumor positions, sizes, and amplitudes of respiration, and another on how accuracy changes when having a fixed body size, a fixed tumor size, and different amplitudes of breathing.

This article serves as an overview of L. Chang, J. Wu et al[6]., the worldwide prevalence of lung cancer, more precisely non-small cell lung cancer, which accounts for 85% of cases of lung cancer and ranks number one in morbidity and cancer-related deaths in 185 nations. Because of their lack of financial and human resources, emerging nations are bearing the brunt of this crisis. Life sciences, massive data sets, and artificial biology are the buzzwords of the 21st century. Here is one of the innovative approaches proposed in the article: building an AI-assisted healthcare system by merging synthetic biology and artificial intelligence. Based on projections of therapy efficacy and economic cost for each individual patient, it customizes drug choices for NSCLC patients.

This is paper introduces RAFENet, H. Li, Q. Song et al[7]., a A novel deep learning model has been developed for the classification of lung cancer subtypes (e.g., adenocarcinoma and squamous cell carcinoma) from CT images. To address the shortcomings of previous methods caused by a lack of training data, this model incorporates an auxiliary image reconstruction task that better represents tumor features. Additionally, it employs a task-aware that encode module with the cross-level non-local hinder to refine features even further, resulting in more accurate classification according to histological subtypes.

This article S. Oh, J.Im et al[8]., describes an attempt to improve the prognosis of non-small cell lung cancer through the use of artificial intelligence. By using the PET scan images of 2,685 non-small cell lung cancer patients, different image feature extracting models were compared within this research. These models include to try to determine the optimal model for estimating the time of survival by comparing accuracy, failure rate, and learning time; these models include ResNet, DenseNet, Efficient Net, and NFNet; and surviving estimation designs, CoxPH and CoxCC.

X. Hu *et al.*, One dependable way to monitor the proliferation of nonsmall cellular lung cancer (NSCLC) is the immunohistochemistry assessment of the Ki67 expression. On the other hand, cancer tissues vary greatly, thus it's possible that a biopsy using a tiny tumor sample is inaccurate. Standard uptake values (SUVs) show low accuracy, even though PET (positron emission tomography) offers a biopsy-free alternative by showing the 3-dimensional functional and anatomical distribution of the cancer cells throughout the whole tumor volume.

The passage addresses the role that precision medicine has played in targeted therapies, particularly radiomics and radiogenomics. The study D. Sui, M. Guo et al[10].,uses radiomics and radiogenomics to analyze medical images for correlation with prognostic and genomic data. Traditional research in this field has already realized high correlations among multi-source medical data, but it results in non-intuitive and non-visual correlation. The paper discusses a deep learning-based radiogenomic framework associating lung tumor image and genomic data, and vice versa. This is a bi-directional framework where, conditional on genomic data, an autoencoder extracts image features for more relevant features than traditional methods.

To increase the accuracy of lung tumor detection, class imbalances can be handled by either oversampling or undersampling or synthetic data generation. Hard negative mining helps narrow down the focus to harder cases and reduce false positives. Decision thresholds can also be adjusted, and techniques such as morphological filtering for post-processing can also be improved upon. In the case of advanced loss functions, attention mechanisms, or domain knowledge added to models such as ResNet-50, U-Net, and VGG-16, this ensures better focus on the critical tumor regions. Collectively, these improvements decrease false positives while maintaining accurate tumor detection, thereby significantly boosting the model's precision.

4.Proposed methodology

In the application of the U-Net model to lung tumor analysis, it uses its encoder-decoder architecture to aid in increasing accuracy in the segmentation of tumours in medical imaging. Convolutional layers with subsequent max-pooling along the encoder path extract high-level features, hence capturing the contextual information about the lung image. The decoder reconstructs the image through up sampling operations, allowing for the introduction of fine details from corresponding encoder layers

through skip connections. Such a dual-path approach enables U-Net to accurately delineate lung tumors of various shapes and dimensions. This will enhance the possibility of early diagnosis and planning for treatment.

The choice of models for lung tumor detection should be clear based on specific use cases, data characteristics, and computational constraints.U-Net is best suited for accurate segmentation tasks due to its encoder-decoder architecture and skip connections, which make it very effective in delineating the boundaries of a tumor. ResNet-50, with its deep residual learning framework, is well-suited for complex feature extraction and classification tasks, especially when high accuracy in distinguishing subtle differences is critical. VGG-16 It is one of the simplest and efficient networks suitable for applications requiring faster computation with moderate accuracy. Its performance can be maximized when model capabilities align with clinical objectives such as segmentation, classification, or efficiency.

1.Data Processing

Collect the lung tumour datasets for input into the U-Net model

1.1 Image Resizing

Resize image to a consistent size

$I_{resized}$=resize (I, (h, w))

Where,

- original image is I .
- height and width of the resized image are h,w.

1.2 Normalization

Normalize pixel values to a range [0,1]

$$I_{norm}=\frac{I-\min(I)}{\max(I)-\min(I)}$$

2.U-Net Architecture

Build the U-Net model, comprising a contacting path, or encoder, and an expansive path, or decoder.

2.1 Contracting Path (Encoder)

2.1.1 Convolution Layer

$$F_{i,j,k}=ReLU(\sum_{m,n}I_{i+m.j+n}.K_{m,n,k}+b_k)$$

Where,

- $F_{i,j,k}$ refers to the map feature.
- Input image is I.
- convolution kernel K and b_k the bias.

2.1.2. Max Pooling Layer

$P_{i,j,k}=\max(F_{2i,2j,k},F_{2i+1,2j,k},F_{2i,2j+1,k},F_{2i+1,2j+1,k})$

2.2 Expansive Path (Decoder)

The image is reconstructed by upsampling and concentrating the data at the decoder.

2.2.1. Up-Convolution Layer

$U_{i,j,k}=UpConv(F_{i,j,k})$

Where UpConv is the up-convolution operation.

2.2.2. Concentration

$C_{i,j,k}=concat(U_{i,j,k},E_{i,j,k})$

Where concat is the merger of the upsampled features maps and the corresponding feature maps from the encoder.

2.2.3. Final Convolution Layer

$\hat{Y}=\sigma(W.C+b)$

Where,

- $\hat{y}$ is the final output.
- W is the mass matrix.
- C stands for the joined feature maps.
- Bias vector denoted by b.
- σ stands for the activation function.

3.Loss Function

Define the loss function by which the model shall be optimized.

3.1 Dice Coefficient Loss

$$\text{Dice Loss}=1-2\frac{\cdot\sum_{i,j}y_{i,j}\hat{y_{i,j}}}{\sum_{i,j}y_{i,j}+\sum_{i,j}\hat{y_{i,j}}}$$

Where,

- y is the ground truth mask.
- $\hat{y}$ is the predict mask.

4.Model Training

Then prepare the U-Net model using an appropriate optimization algorithm.

4.1 Gradient Descent

Update the model parameters with the loss minimum.

$\theta=\theta-\alpha\nabla_\theta Loss$

Where,θ is a collection of model parameters, α is the rate of learning and $\nabla_\theta Loss$ is the loss of gradient with respect to θ.

To enhance the precision of the proposed lung tumor detection methods, several strategies can be used. Data augmentation techniques, including rotation, scaling, and contrast adjustments, can be used to increase model robustness by diversifying

the training data. Hyperparameter optimization and k-fold cross-validation ensure better model generalization and performance. The combination of ensemble learning brings the strengths of ResNet-50, U-Net, and VGG-16 together to further improve diagnostic precision. The third one is that transfer learning with pre-trained weights may handle issues with small datasets, while error analysis and targeted refinements in loss functions can address misclassifications. Collectively, these improvements make lung tumor diagnosis more reliable and accurate for clinical use.

Normalization ensures that data is scaled consistently, which means the model trains more stably and performs better. For lung tumor detection, pixel values can be rescaled to a range of [0, 1] or standardized using mean and standard deviation (mean normalization). In RGB images, each channel is normalized independently. For medical images like CT scans, Z-score normalization (zero mean, unit variance) is often applied to handle high dynamic ranges. Consistency in normalization when training as well as inferring leads to better convergence and accurate models.

5.Results

For instance, in lung tumor segmentation, there are some performance differences for variants of the U-Net, such as U-Net ResNet-50 and U-Net VGG-16. To that effect, U-Net ResNet-50 demonstrates better accuracy and robustness for the segmentation of complex tumor structures, able to handle multiple tumor sizes and shapes efficiently. On the other hand, U-Net VGG-16 has simplicity and efficiency as its major features, hence giving faster computation times with a little reduction in segmentation precision. Overall, for very high accuracy needed in an application, U-Net ResNet-50 will be more appropriate, while in situations where computational efficiency maximization is required, U-Net VGG-16 is more applicable.

TABLE 1

Accuracy Comparison

No of samples	ResNet-50	U-Net	VGG-16
100	0.86	0.81	0.82
200	0.87	0.83	0.83
300	0.88	0.84	0.84
400	0.89	0.85	0.85
500	0.90	0.87	0.86
600	0.91	0.89	0.87

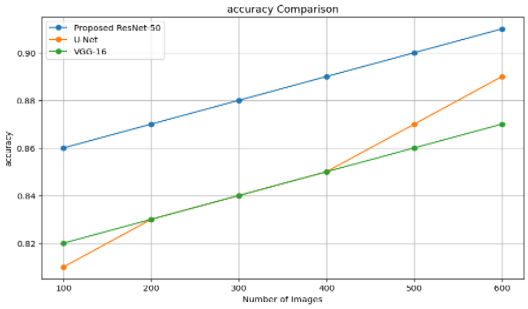

Fig 2- Accuracy comparison

The above table1 and fig2 shows the subtotals of accuracy of 3models.The proposed ResNet-50 obtained the maximum accuracy when compared to other configurations such as VGG-16 and U-Net.

TABLE 2

Precision Comparison

No of samples	ResNet-50	U-Net	VGG-16
100	0.85	0.81	0.80
200	0.86	0.82	0.81
300	0.87	0.84	0.82
400	0.88	0.85	0.83
500	0.89	0.86	0.84
600	0.90	0.88	0.85

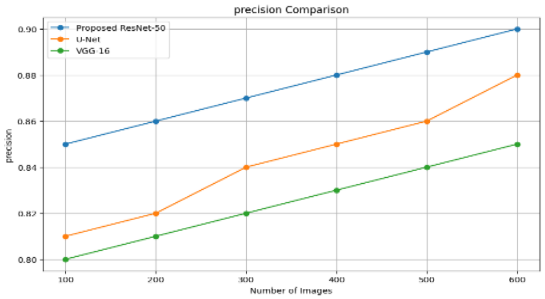

Fig 3- Precision comparison

The above table 2 and fig 3 shows that proposed ResNet-50 for every count of image it obtains significantly improved precision when compared to U-Net and VGG-16.

TABLE 3

Recall Comparison

No of samples	ResNet-50	U-Net	VGG-16
100	0.84	0.81	0.82
200	0.85	0.83	0.83
300	0.86	0.85	0.85
400	0.88	0.87	0.86
500	0.90	0.89	0.87
600	0.91	0.90	0.88

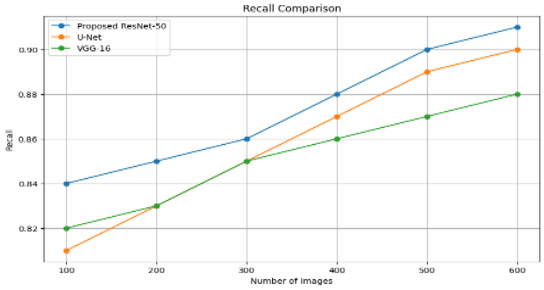

Fig 4-Recall comparison

The above table3 and fig4 shows that proposed ResNet-50 performs slightly better than U-Net but a lot better than VGG-16. The recall comparison increases when the number of images rises from 100-600 at every level. As the number of images increases from 100-600 the models are learned better.

TABLE 4

F1 Score Comparison

No of samples	ResNet-50	U-Net	VGG-16
100	0.81	0.80	0.81
200	0.83	0.82	0.82
300	0.85	0.84	0.83
400	0.87	0.85	0.84
500	0.89	0.86	0.85
600	0.91	0.89	0.86

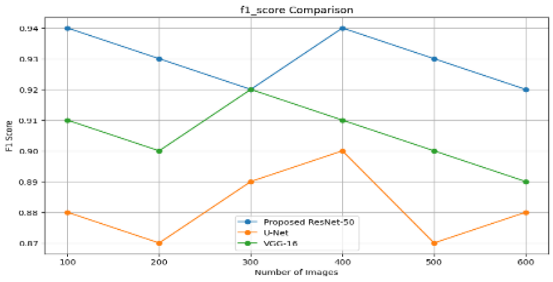

Fig 5-f1 score comparison

The above table4 and fig5 reveals the F1 score difference margins of 3 models namely ResNet-50 and the next best U-Net and then VGG-16.

TABLE 5

Computation Time Comparison

No of samples	ResNet-50	U-Net	VGG-16
100	0.5	0.2	0.4
200	0.6	0.4	0.5
300	0.7	0.6	0.6
400	0.8	0.8	0.7
500	0.9	0.10	0.9
600	0.11	0.12	0.10

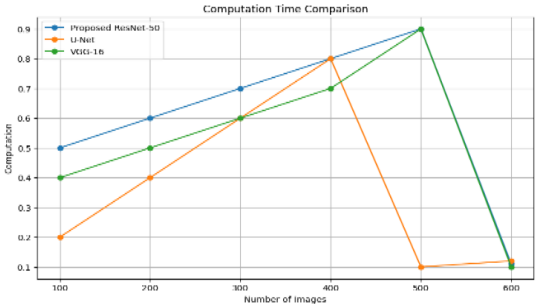

Fig 5-Computation comparison

The above table5 and fig5 shows comparison of processing time of Proposed ResNet-50, U-Net and VGG-16 in terms of the number of images ranging from 100 to 600.Proposed MS-CNN gives the shortest processing time. As the number of images increases, both recognition rate and computation time of all models also increase.

The above tables and graphs show the results of accuracy and time taken by the Proposed ResNet-50 with the U-Net and VGG-16 on image count. It has been observed that Proposed ResNet-50 performs better than other models in terms of accuracy and time complexity, followed by the U-Net and VGG-16 model. The accuracy of all models increases with more numbers of the image it require more time as the number of images increases. Finally concluded that Proposed ResNet-50 is more accurate as well as efficient.

6. Conclusion

These results of the study prove that ResNet-50, U-Net, and VGG-16 algorithms show a highly significant improvement in the lung tumor detection performance metrics. The comprehensive and robust framework for lung tumor analysis is provided only when ResNet-50 deep residual learning, U-Net excellent image segmentation, and VGG-16 robust convolutional features are combined. The improved diagnostic performance metrics seen in this study suggest that these deep learning models can aid effectively in clinical diagnosis toward an accurate and timely diagnosis of lung cancer.

Further, the algorithms are said to be computationally efficient and, therefore, feasible for real-world medical application in which speed and reliability in diagnoses are critical. These sophisticated algorithms increase the precision and reliability of lung tumor detection and support treatment plans by providing detailed and accurate diagnostic information. This computational oncology development could greatly enhance patient outcomes by facilitating an earlier and more accurate diagnosis of lung tumors, enabling appropriate treatments with better survival rates.

These results indicate a critical role that deep learning could play in improving oncology diagnostics and, therefore, further research and development. Diagnosis with higher standards of accuracy can be performed by use of the strengths in ResNet-50, U-Net, and VGG-16 in achieving diagnostic accuracy, hence improving the general care and management of the patients in lung cancer treatment.

References

[1] Q. -L. Lian, X. -Y. Li, B. Lu, C. -W. Zhu, J. -T. Li and J. -J. Chen, "Identification of Lung Tumors in Nude Mice Based on the LIBS With Histogram of Orientation Gradients and Support Vector Machine," in *IEEE Access*, vol. 11, pp. 141915-141925, 2023, doi: 10.1109/ACCESS.2023.3342105.

[2] H. Hu, Q. Li, Y. Zhao and Y. Zhang, "Parallel Deep Learning Algorithms With Hybrid Attention Mechanism for Image Segmentation of Lung Tumors," in *IEEE Transactions on Industrial Informatics*, vol. 17, no. 4, pp. 2880-2889, April 2021, doi: 10.1109/TII.2020.3022912.

[3] P. Yin, B. Hu, Q. Li, Y. Duan and Q. Lin, "Imaging of Tumor Boundary Based on Multielements and Molecular Fragments Heterogeneity in Lung Cancer," in *IEEE Transactions on Instrumentation and Measurement*, vol. 70, pp. 1-7, 2021, Art no. 4006207, doi: 10.1109/TIM.2021.3102755.

[4] H. Ladjal, M. Beuve, P. Giraud and B. Shariat, "Towards Non-Invasive Lung Tumor Tracking Based on Patient Specific Model of Respiratory System," in *IEEE Transactions on Biomedical Engineering*, vol. 68, no. 9, pp. 2730-2740, Sept. 2021, doi: 10.1109/TBME.2021.3053321.

[5] T. Peng, Z. Jiang, Y. Chang and L. Ren, "Real-Time Markerless Tracking of Lung Tumors Based on 2-D Fluoroscopy Imaging Using Convolutional LSTM," in *IEEE Transactions on Radiation and Plasma Medical Sciences*, vol. 6, no. 2, pp. 189-199, Feb. 2022, doi: 10.1109/TRPMS.2021.3126318.

[6] L. Chang, J. Wu, N. Moustafa, A. K. Bashir and K. Yu, "AI-Driven Synthetic Biology for Non-Small Cell Lung Cancer Drug Effectiveness-Cost Analysis in Intelligent Assisted Medical Systems," in *IEEE Journal of Biomedical and Health Informatics*, vol. 26, no. 10, pp. 5055-5066, Oct. 2022, doi: 10.1109/JBHI.2021.3133455.

[7] H. Li, Q. Song, D. Gui, M. Wang, X. Min and A. Li, "Reconstruction-Assisted Feature Encoding Network for Histologic Subtype Classification of Non-Small Cell Lung Cancer," in *IEEE Journal of Biomedical and Health Informatics*, vol. 26, no. 9, pp. 4563-4574, Sept. 2022, doi: 10.1109/JBHI.2022.3192010.

[8] S. Oh, J. Im, S. -R. Kang, I. -J. Oh and M. -S. Kim, "PET-Based Deep-Learning Model for Predicting Prognosis of Patients With Non-Small Cell Lung Cancer," in *IEEE Access*, vol. 9, pp. 138753-138761, 2021, doi: 10.1109/ACCESS.2021.3115486.

[9] X. Hu *et al.*, "3-D Textural Analysis of 2-[^{18}F]FDG PET and Ki67 Expression in Nonsmall Cell Lung Cancer," in *IEEE Transactions on Radiation and Plasma Medical Sciences*, vol. 6, no. 1, pp. 113-120, Jan. 2022, doi: 10.1109/TRPMS.2021.3051376.

[10] D. Sui, M. Guo, X. Ma, J. Baptiste and L. Zhang, "Imaging Biomarkers and Gene Expression Data Correlation Framework for Lung Cancer Radiogenomics Analysis Based on Deep Learning," in *IEEE Access*, vol. 9, pp. 125247-125257, 2021, doi: 10.1109/ACCESS.2021.307146.

[11] T. Xu, P. Zhang, Q. Huang, H. Zhang, Z. Gan, X. Huang, et al., "AttnGAN: Fine-grained text to image generation with attentional generative adversarial networks", *Proc. IEEE Conf. Comput. Vis. Pattern Recognit.*, pp. 1316-1324, Jun. 2018.

[12] M. Zhou, A. Leung, S. Echegaray, A. Gentles, J. B. Shrager, K. C. Jensen, et al., "Non–small cell lung cancer radiogenomics map identifies relationships between molecular and imaging phenotypes with prognostic implications", *Radiology*, vol. 286, no. 1, 2017.

[13] A.B. L. Larsen, S. K. Sønderby, H. Larochelle and O. Winther, "Autoencoding beyond pixels using a learned similarity metric" in arXiv:1512.09300, 2015, [online] Available: http://arxiv.org/abs/1512.09300.

[14] S. Dong, G. Luo, K. Wang, S. Cao, A. Mercado, O. Shmuilovich, et al., "VoxelAtlasGAN: 3D left ventricle segmentation on echocardiography with atlas guided generation and voxel-to-voxel discrimination" in arXiv:1806.03619, 2018, [online] Available: http://arxiv.org/abs/1806.03619.

[15] H. Uzunova, J. Ehrhardt and H. Handels, "Memory-efficient GAN-based domain translation of high resolution 3D medical images", *Comput. Med. Imag. Graph.*, vol. 86, Dec. 2020.

[16] D. Jin, Z. Xu, Y. Tang, A. P. Harrison and D. J. Mollura, "CT-realistic lung nodule simulation from 3D conditional generative adversarial networks for robust lung segmentation", *Proc. Int. Conf. Med. Image Comput. Comput.-Assist. Intervent.*, pp. 732-740, 2018.

[17] J. Johnson, A. Alahi and L. Fei-Fei, "Perceptual losses for real-time style transfer and super-resolution", *Proc. Eur. Conf. Comput. Vis*, pp. 694-711, 2016.

[18] O. Gevaert, J. Xu, C. D. Hoang, A. N. Leung, Y. Xu, A. Quon, et al., "Non–small cell lung cancer: Identifying prognostic imaging biomarkers by leveraging public gene expression microarray data—methods and preliminary results", *Radiology*, vol. 264, no. 2, pp. 387-396, Aug. 2012.

[19] H. Abdollahi, S. Mostafaei, S. Cheraghi, I. Shiri, S. R. Mahdavi and A. Kazemnejad, "Cochlea CT radiomics predicts chemoradiotherapy induced sensorineural hearing loss in head and neck cancer patients: A machine learning and multi-variable modelling study", *Phys. Medica*, vol. 45, pp. 192-197, Jan. 2018.

[20] T. Schlegl, P. Seeböck, S. M. Waldstein, U. Schmidt-Erfurth and G. Langs, "Unsupervised anomaly detection with generative adversarial networks to guide marker discovery", *Proc. Int. Conf. Inf. Process. Med. Imag.*, pp. 146-157, 2017.

[21] J. Xu, L. Xiang, Q. Liu, H. Gilmore, J. Wu, J. Tang, et al., "Stacked sparse autoencoder (SSAE) for nuclei detection on breast cancer histopathology images", *IEEE Trans. Med. Imag.*, vol. 35, no. 1, pp. 119-130, Jan. 2016.

[22] A.V. Dalca, J. Guttag and M. R. Sabuncu, "Anatomical priors in convolutional networks for unsupervised biomedical segmentation", *Proc. IEEE Conf. Comput. Vis. Pattern Recognit.*, pp. 9290-9299, Jun. 2018.

[23] H. Dong, G. Yang, F. Liu, Y. Mo and Y. Guo, "Automatic brain tumor detection and segmentation using U-Net based fully convolutional networks", *Proc. Annu. Conf. Med. Image Understand. Anal.*, pp. 506-517, 2017.

[24] F. Milletari, N. Navab and S.-A. Ahmadi, "V-Net: Fully convolutional neural networks for volumetric medical image segmentation", *Proc. 4th Int. Conf. 3D Vis.*, pp. 565-571, Oct. 2016.

[25] T. P. Coroller, P. Grossmann, Y. Hou, E. Rios Velazquez, R. T. H. Leijenaar, G. Hermann, et al., "CT-based radiomic signature predicts distant metastasis in lung adenocarcinoma", *Radiotherapy Oncol.*, vol. 114, no. 3, pp. 345-350, Mar. 2015.